TRENDS IN SCIENCES 2026; 23(9): 12663
https://doi.org/10.48048/tis.2026.12663 RESEARCH ARTICLE

Cinnamaldehyde-Chitosan Nanoparticles Protect Fibroblasts from High-Glucose-Induced Apoptosis via PI3K/AKT Pathway Activation

Editya Fukata[1,2], Mohammad Saifur Rohman[3,4], Aulanniam[5], Husnul Khotimah[6], Nik Ahmad Nizam Nik Malek[7] and Agustina Tri Endharti[8,9,*]

[1]Doctoral Program in Medical Science, Faculty of Medicine, Universitas Brawijaya, Malang, Indonesia
[2]Department of Medicine, Faculty of Medicine, Universitas Negeri Malang, Malang, Indonesia
[3]Department of Cardiology and Vascular Medicine, Faculty of Medicine, Universitas Brawijaya-Saiful Anwar General Hospital, Malang, Indonesia
[4]Cardiovascular Research Centre, Universitas Brawijaya, Malang, Indonesia
[5]Department of Chemistry, Faculty of Sciences, Universitas Brawijaya, Malang, Indonesia
[6]Department of Pharmacology, Faculty of Medicine, Universitas Brawijaya, Malang, Indonesia
[7]Universiti Teknologi Malaysia, Centre for Sustainable Nanomaterials (CSNano), Universiti Teknologi Malaysia, Johor Bahru, Malaysia
[8]Department of Parasitology, Faculty of Medicine, Universitas Brawijaya, Malang, Indonesia
[9]Biomedical Central Laboratory, Faculty of Medicine, Universitas Brawijaya, Malang, Indonesia

([*]Corresponding author's e-mail: tinapermana.fk@ub.ac.id)

Received: 15 November 2025, Revised: 18 December 2025, Accepted: 28 December 2025, Published: 20 March 2026

Abstract

Hyperglycemia disrupts wound healing in diabetes partly by promoting fibroblast apoptosis. This study aimed to evaluate whether cinnamaldehyde-chitosan nanoparticles (CCNPs) can inhibit high-glucose-induced fibroblasts apoptosis, and to determine whether this effect involves modulation of the PI3K/AKT pathway. CCNPs were synthesized using a modified ionic-gelation method and characterized by Dynamic Light Scattering (DLS) and Transmission Electron Microscopy (TEM). Murine embryonic fibroblasts cell line (NIH-3T3) were allocated to 6 groups: 2 control groups - normal glucose (NG, 5.5 mM glucose) and high glucose (HG, 30 mM glucose) - and 4 treatment groups that were pretreated with metformin (50 µM) or CCNPs (12.5, 25 and 50 µM) prior to 24 h of HG exposure. After 24 h of treatment, PI3K and phosphorylated-AKT levels in the cell lysates were quantified using ELISA, and fibroblasts apoptosis was assessed and quantified by Annexin V-PI flow cytometry. Synthesized CCNPs exhibited spherical morphology with an average diameter of 214.8 ± 54.0 nm, a polydispersity index (PDI) of 0.419, and a ζ-potential of +66.2 mV. High glucose exposure significantly increased the proportion of late apoptotic cells and reduced PI3K and p-AKT expression, compared with NG group ($p < 0.05$). Meanwhile, CCNPs at all tested concentrations significantly reduced late apoptotic cell percentages in a concentration-dependent manner, whereas only CCNPs at 50 µM significantly restored both PI3K and p-AKT levels. These findings suggest that CCNPs mitigate high-glucose-induced fibroblast apoptosis and is likely associated with the activation of PI3K/AKT pathway. This study provides preliminary in vitro evidence supporting a potential fibroblast-protective role of CCNPs under hyperglycemic conditions. Limitations of this study include the short-term *in-vitro* design and the absence of a direct comparison between CCNPs versus cinnamaldehyde only. Future studies should incorporate longer exposure durations, pathway-specific inhibitor, and *in-vivo* validation.

Keywords: Apoptosis, Cinnamaldehyde, Fibroblast, High glucose, Chitosan nanoparticle, PI3K, AKT

Introduction

Diabetes mellitus remains a major global health issue, affecting over 500 million adults worldwide and its prevalence is projected to rise by 46% by 2050 [1]. Chronic hyperglycemia is the main pathological feature of diabetes and contributes to the development of numerous complications through multiple mechanisms involving oxidative stress, inflammation, and cellular apoptosis [2]. Fibroblasts play a pivotal role in maintaining the structural integrity of tissues by synthesizing extracellular matrix components (ECM) and facilitating tissue repair; thus, increased fibroblast apoptosis has been associated with delayed tissue repair and impaired wound healing commonly observed in diabetic patients [3,4]. Current standard management of diabetic wounds primarily focuses on correcting contributory systemic and local factors - such as ischemia, pressure, infection, and hyperglycemia - alongside optimized local wound care. While these strategies indirectly support fibroblast function by improving the wound microenvironment, they do not specifically target hyperglycemia-induced fibroblast dysfunction or apoptosis [5]. In contrast, emerging preclinical approaches aimed at directly correcting fibroblast-specific molecular abnormalities, including growth factor-based therapies [6] and gene-modulating strategies (e.g., PDK4-related interventions) [7], have demonstrated promising improvements in diabetic wound healing outcomes, underscoring the therapeutic potential of fibroblast-targeted strategies.

Hyperglycemia induces excessive reactive oxygen species (ROS) generation and disrupts redox balance, leading to mitochondrial dysfunction and subsequent activation of pro-apoptotic signaling cascades [8]. Additionally, hyperglicemia enhances the formation of oxidized advanced glycation end-products (AGE) which further aggravate oxidative stress and inhibit fibroblasts proliferation [9]. The phosphatidylinositol-4,5-bisphosphate 3-kinase (PI3K)/protein kinase B (AKT) signaling pathway is crucial for both glucose metabolism and cell survival, and its downregulation under hyperglycemic stress has been observed to promote apoptosis in multiple cell types, including fibroblasts [10-13]. Therefore, therapeutic strategies aimed at restoring PI3K/AKT signaling may hold promise for preventing fibroblast apoptosis and improving diabetic wound healing.

Cinnamaldehyde (CA), the major bioactive compound in *Cinnamomum* spp. bark essential oils, has been reported to possess anti-inflammatory, antioxidant, antidiabetic, and antimicrobial properties [14-16]. CA is a naturally occurring antioxidant that has been demonstrated to mitigate oxidative stress by scavenging free radicals and activating endogenous antioxidant systems by modulating several intracellular signaling pathways, such as nuclear factor erythroid 2–related factor 2 (Nrf2) and PI3K/AKT [17-19]. CA has been reported to upregulate the expression of PI3K/AKT pathway key components, including insulin receptor substrate-1 (IRS-1), phosphorylated PI3K and AKT in myocardial hypoxia model in vitro [18], and in streptozotocin-induced diabetic rats [20]. The upregulation of these pro-survival pathways contributes to the inhibition of the apoptotic cascade and subsequent reduction of apoptosis, as supported by previous experimental studies [18,21]. Complementing these findings, in silico studies suggest potential direct interactions between CA and PI3K/AKT proteins; however, these computational predictions have yet to be experimentally validated, and the precise molecular mechanisms remain incompletely defined [22]. Collectively, this body of evidence suggest that CA is a promising candidate for preventing high-glucose-induced fibroblast apoptosis.

Despite its considerable therapeutic potential, the clinical application of CA remains limited due its susceptibility to oxidation, poor aqueous solubility, high volatility, and mucosal irritative properties, which collectively might reduce its oral tolerability, bioavailability and stability [16,23,24]. Nanotechnology-based drug delivery systems have emerged as a powerful strategy to overcome such pharmacokinetic limitations. Chitosan, a naturally derived biopolymer, offers excellent biocompatibility, biodegradability, and mucoadhesive properties, making it a suitable carrier for CA [25,26]. The formulation of cinnamaldehyde-chitosan nanoparticles (CCNPs) have been shown to enhance the stability, solubility, and controlled release of CA. Moreover, experimental evidence suggests that chitosan encapsulation protects CA degradation, increasing its local concentration at

target surfaces and enabling sustained release, which may contribute to enhanced antimicrobial efficacy [27-29]. Reduced degradation also preserves CA's radical-scavenging capacity for longer durations compared with free CA [27]. In addition, prior studies revealed that CA encapsulation reduces cytotoxic effects observed at higher CA concentrations in human oral epithelial cells, indicating a protective role of chitosan-based nanoformulation [30].

Taken together, the intrinsic antioxidant properties and potential modulation of the PI3K/AKT signaling pathway by CA, combined with the pharmacokinetic advantages conferred by chitosan nanoencapsulation, suggest that CCNPs may effectively mitigate fibroblast apoptosis under hyperglycemic conditions. However, despite growing evidence supporting the individual anti-apoptotic potential of CA [17-19] and the benefits of chitosan-based nanoformulations [27-29], the effects of CCNPs on fibroblast apoptosis in a hyperglycemic environment have not been systematically investigated. In particular, it remains unclear whether nanoencapsulation of CA enhances its ability to restore PI3K/AKT signaling and protect fibroblasts from high-glucose-induced apoptosis.

Therefore, this study tested the hypothesis that CCNPs attenuate high-glucose-induced fibroblast apoptosis and is associated with activation of the PI3K/AKT signaling pathway. The specific aims were to (1) evaluate the anti-apoptotic effects of CCNPs and (2) determine the effects of CCNPs on PI3K and p-AKT levels in a hyperglycemic NIH-3T3 fibroblast model.

Materials and methods

Cell culture

NIH-3T3 immortalized mouse embryonic fibroblasts (ATCC, CRL-1658, Virginia, USA) were used for all experiments. Cells were maintained in polystyrene culture flasks containing Dulbecco's Modified Eagle Medium (Gibco, Missouri, USA) with 5.5 mM glucose, supplemented with 10% fetal bovine serum (FBS) and 1% penicillin-streptomycin, and incubated at 37 °C in humidified 5% CO_2. Cells were subcultured every third day using trypsin-EDTA. All experiments were conducted using cells at passages 10 - 15. The cell line had undergone routine authentication and mycoplasma testing by ATCC prior to distribution; no additional authentication or mycoplasma testing was performed in our laboratory.

Nanoparticle synthesis and characterization

Cinnamaldehyde-chitosan nanoparticles were synthesized using the ionic gelation method based on previous studies, with several modifications [28,29]. Chitosan derived from shrimp shells (Sigma-Aldrich, Cat# C3646, Lot# SLBW1036), with a degree of deacetylation ≥ 75 % and a medium molecular weight (190 - 375 kDa), was used as the polymeric carrier. Briefly, 200 mg of chitosan was dissolved in 100 mL of 1% (v/v) acetic acid and homogenized by magnetic stirring at 60 °C to obtain a final concentration of 2 mg/mL. To reduce polymer size and enhance nanoparticle uniformity, the solution was stirred overnight at 60 °C, followed by sequential filtration through standard filter paper and a 0.4 μm microfilter to remove residual aggregates. The filtrate was then subjected to ultrasonication for 2 h to further improve chitosan dispersion prior to nanoparticle formation.

Next, sodium tripolyphosphate (STPP) solution was prepared by dissolving 40 mg of analytical-grade STPP (Xilong Scientific, Guangdong, China) in 40 mL of distilled water. The STPP solution was added dropwise to the chitosan solution under continuous stirring for 1 h at 60 °C until completely dissolved (chitosan-TPP volume ratio 1:1). Cinnamaldehyde (CA) suspension was made by dissolving cinnamaldehyde (≥ 95% purity, SigmaAldrich, Cat#W228613, Missouri, USA) in ethanol (25%, v/v) to obtain a final concentration of 1%. Subsequently, 20 mL of the 1% CA solution was added dropwise into the prepared chitosan-TPP mixture and stirred at 60 °C until a homogeneous suspension was obtained (CA:Chitosan-STPP ratio 1:4). The final concentration of CCNPs obtained was 2 mg/mL (~15 mM). Encapsulation efficiency and drug loading capacity were not quantified in the present study. The CCNPs suspension was then analyzed by dynamic light scattering using Horiba-SZ 100z Particle Size Analyzer (ILRC UI, Jakarta, Indonesia) to determine the average particle size, polydispersity index (PDI) and Zeta potential. The morphological characteristics of the nanoparticles were confirmed by transmission electron microscopy (Jeol JEM-1400, Japan).

Experimental design

NIH-3T3 cells were cultured in DMEM supplemented as described above until approximately 80% confluence was reached. Cells were then equally and randomly assigned to 6 experimental groups: normal glucose (NG, 5.5 mM glucose), high glucose (HG, 30 mM glucose) as the positive control group, metformin-treated group (M, 50 μM), and 3 CCNP-treated groups (12.5, 25 and 50 μM). High-glucose conditions were established by supplementing DMEM with D-glucose to a final concentration of 30 mM, based on previous studies [12,31,32]. CCNPs or metformin (50 μM) were administered 2 h prior to HG exposure, followed by incubation under HG conditions for 24 h. Three technical replicates (3 wells per group, n = 3) were used for each experiment, and each downstream assay was performed using a separate set of culture plates. Blinding was not applied in present study.

Cell morphology observation

NIH-3T3 cells were seeded in a 6-well plate. After 24 h of incubation with either NG or HG, the cells were stained using Trichrome staining, following protocol described in previous study [33]. The morphology of the cells was examined and documented using an inverted microscope at 200× and 400× magnifications.

PI3K and p-AKT measurement

NIH-3T3 cells (1×10^5 cells/well) were seeded in 12-well plates containing complete medium. Upon reaching 80% confluence, cells were treated according to their assigned experimental groups. After 24 h of incubation, cell lysates were prepared by adding 200 μL of RIPA lysis & extraction buffer (G-Biosciences, Cat#786-489, Missouri, USA) to each well, followed by incubation on ice for 15 minutes with periodic pipetting. Cell homogenates were collected using cell scraper, transferred to microcentrifuge tubes, and centrifuged at 14,000×g for 15 min. After that, the supernatant was carefully pipetted and transferred to new microcentrifuge tubes. Intracellular PI3K and phosphorylated AKT (p-AKT) levels were then measured using sandwich enzyme-linked immunosorbent assay (ELISA) kits (BT LAB; PI3K Cat#E0438Mo, Lot#202309016; p-AKT Cat#E1201Mo, Lot#202309016) according to the manufacturers' instructions. The color absorbance was measured by ELISA microplate reader at a wavelength of 450 nm.

Apoptosis measurement

Apoptosis was assessed using the Annexin V-FITC Apoptosis Detection Kit (BioLegend, Cat#640914, Lot#B258536, California, USA) in accordance with the recommended protocol. NIH-3T3 cells were seeded in 6-well plates (1×10^6 cells per well). After 24 h of treatment, the cells were incubated with trypsin-EDTA for 7 min to detach the cells and then centrifuged at 2,000 rpm for 5 min. Cell pellets were obtained and resuspended in 100 μL of binding buffer, followed by the addition of 5 μL of Annexin V-FITC and 5 μL of propidium iodide (PI). Samples were gently mixed and incubated for 15 min at room temperature in the dark.

Flow cytometric analysis was performed using a BD FACSCalibur™ flow cytometer with BD CellQuest Pro™ software. First, cell debris and doublets were excluded using FSC/SSC and singlet gating. On the compensated data from the debris-free singlets, Annexin V-FITC versus PI dot plots were used to define quadrants corresponding to viable, early apoptotic, late apoptotic, and necrotic cells. Percentages of cells in each population were calculated.

Statistical analysis

The data obtained from the experiments were analyzed using SPSS software version 25 (New York, USA) and visualized using GraphPad Prism version 9.0 (Boston, USA). The results are presented as mean ± standard deviation (SD) from 3 technical replicates. Normality and homogeneity of variance were assessed using the Kolmogorov-Smirnov test and Levene's test, respectively. As data met the assumptions of normality and homogeneity, comparisons among multiple groups were performed using 1-way analysis of variance (ANOVA), followed by Tukey's post-hoc test for pairwise comparisons. No missing data were observed, and all samples were included in the final analysis. p values < 0.05 were considered significant.

Results and discussion

Characterization of cinnamaldehyde-chitosan nanoparticles (CCNPs)

Dynamic Light Scattering (DLS) analysis was conducted to determine the average diameter, poly dispersity index (PDI), and surface charge (ζ-potential) of the CCNPs (**Figures 1(A)** and **1(B)**). CCNPs showed a particle size diameter of 214.8 ± 54.0 nm, with a PDI value of 0.419 and ζ-potential of +66.2 mV. The sample exhibited a single peak curve, which indicates uniform particle size distribution. A narrower curve showed better results in terms of particle size uniformity. CCNPs' morphology was further visualized using TEM (**Figures 1(C)** and **1(D)**). Synthesized CCNPs were well-dispersed and exhibited a spherical structure and smooth surface, confirming their vesicular nature and lamellarity characteristics. TEM micrograph also showed smaller average diameter (53.19 ± 29 nm) than that obtained from DLS measurements. This variation is likely attributed to particle shrinkage during the sample preparation process for TEM analysis [27].

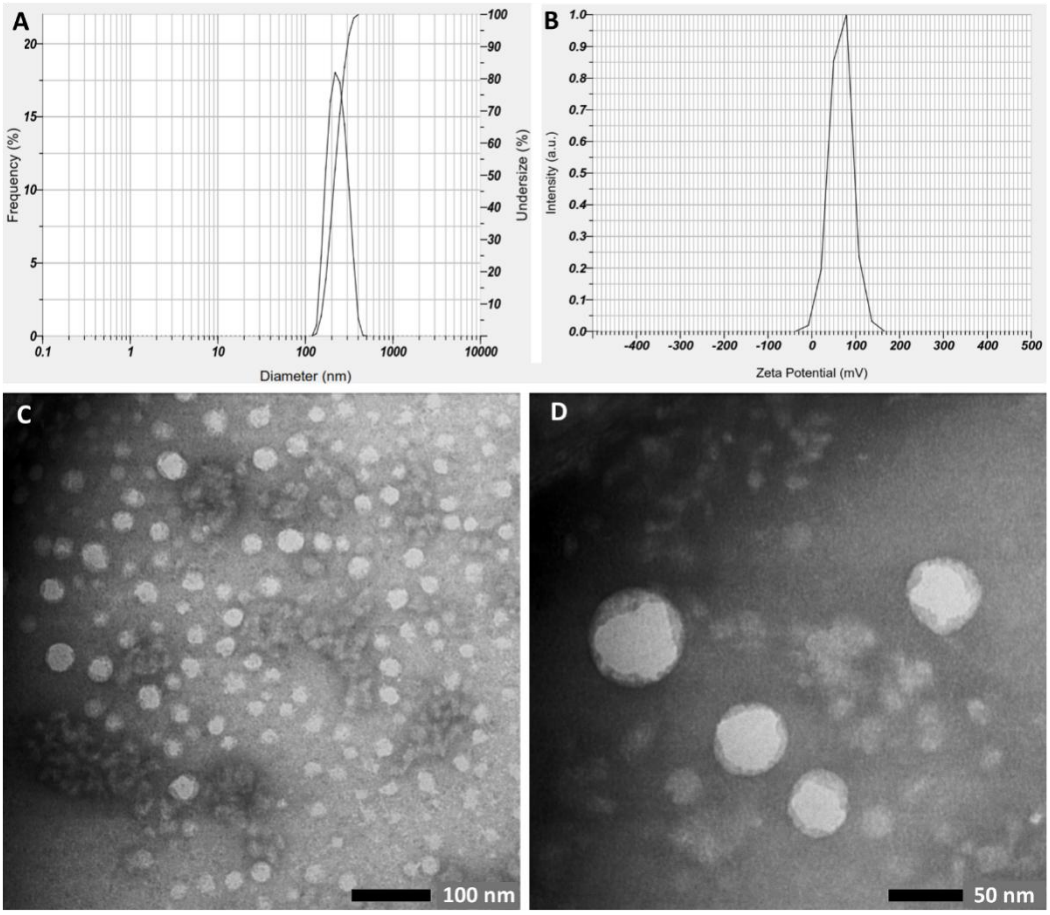

Figure 1 Characterization of synthesized CCNPS based on (A) size distribution, (B) ζ-potential, and (C, D) TEM analysis (at 40,000× and 80,000× magnification, respectively).

Encapsulation of bioactive compound with nano-sized particles will improve its stability, increase the bioavailability and absorption, as well as maintain the efficacy of the drug compounds [34]. Biopolymer-based nanoparticles, including chitosan, have been utilized to improve the pharmacokinetics of CA. CCNPs synthesized with ionic gelation method have been reported to achieve an encapsulation efficiency of 39.7% - 90% with an average particle size of 166 - 455 nm, and a fairly variable zeta potential from −40 mV to +65 mV [27-29,35-37]. Present study reported similar results. Nano-sized particles have been achieved because the particles size falls within the nanoscale range of 1 - 500 nm (214.8 ± 54.0 nm). Particle size is a critical parameter, as it influences the characteristics, stability, and potential applications of the delivery

systems. A smaller average particle size facilitates rapid diffusion and swift release of core materials, whereas larger particles delay the release of bioactive compounds due to their increased interfacial area thus providing a more sustained release [38]. Interestingly, TEM images showed a smaller average diameter of CCNPs (53.19 ± 29 nm). This variation is likely attributed to particle shrinkage during the sample preparation process for TEM analysis [27]. Our formulation resulted in a low PDI value (0.419), indicating a homogenous sample in terms of its particle size [39]. It is further confirmed by the TEM results which showed that the CCNPs were well-dispersed and exhibited a uniformity in terms of structure and surface. Furthermore, the high absolute ζ-potential value indicates highly charged particles that will prevent aggregation due to the strong repulsive forces between particles. As a general rule, nanoparticles with absolute ζ-potential value between 30 - 60 mV is considered to have good stability [40]. Differences in these parameters are strongly influenced by the biopolymer composition, namely the chitosan concentration and chitosan:STPP ratio, and the encapsulation method used[41]. Nevertheless, previous research results demonstrated that chitosan nanoparticles showed high encapsulation efficiency and provided sustained release of CA [35,36].

High-glucose exposure induced morphological changes in NIH-3T3 cells

High-glucose exposure induced NIH-3T3 cell injury as indicated by morphological observation. Morphological observation using light inverted microscopy showed several characteristic features that differ between NG and HG groups (**Figure 2**). NIH-3T3 cells in the HG group had large nuclei with prominent nucleoli. Additionally, abundant cytoplasm and numerous cytoplasmic processes were also observed among the characteristic features. In general, NIH-3T3 cells in the HG group were found to be larger compared to those of the NG group, suggesting cellular hypertrophy. Previous reports have shown that high glucose promotes fibroblast hypertrophy, characterized by increased cell size and protein content, which might be attributed to cellular response to stress induced by a high-glucose environment [32,42]. In support with our findings, apoptotic cells have also been described to exhibit an apparent increase in surface area during apoptotic body formation, a process requiring membrane expansion and cell rounding to facilitate fragmentation [43].

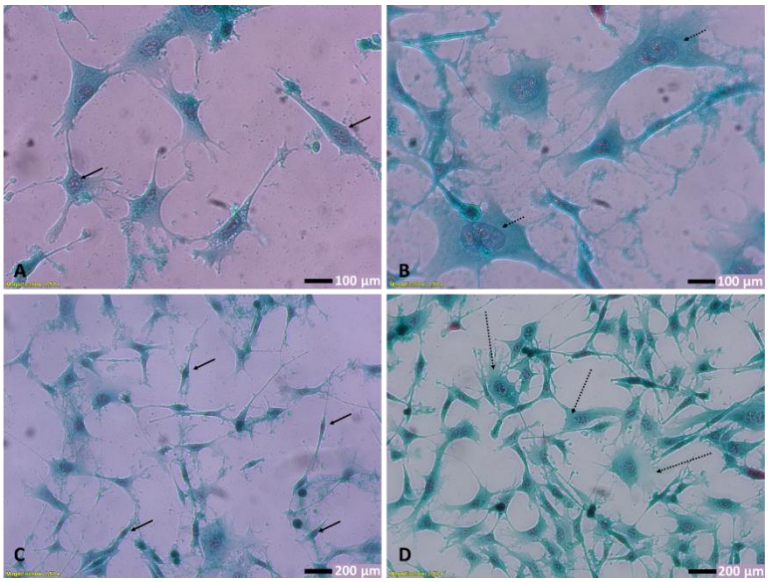

Figure 2 Effect of high-glucose exposure on NIH-3T3 cells morphology. (A,C) Cells in NG group, observed in 400× and 200× magnification, respectively. Cells in NG group showed spindle shape fibroblasts with few cytoplasmic extensions and rounded to oval nuclei with one or 2 nucleoli (arrows). (B,D) Cells in HG group, observed in 400× and 200× magnification. Notice satellite and pyramidal-shaped fibroblasts (dotted arrows) with numerous finger-like cytoplasmic protrusions (filopodia). All photos were taken 24 h after exposure to either NG or HG media.

CCNPs attenuated apoptosis and upregulated PI3K/AKT pathway in HG-treated NIH-3T3

To date, the application of cinnamaldehyde–chitosan nanoparticles (CCNPs) has largely been confined to the food industry due to their recognized antimicrobial and antioxidant properties [26,27,44]. To our knowledge, this is the first study to investigate the protective effects of CCNPs against high-glucose induced fibroblast apoptosis. In this study, NIH-3T3 fibroblasts were pre-treated with CCNPs or metformin, followed by exposure to 30 mM D-glucose to mimic hyperglycemic conditions observed in diabetic patients.

As shown in **Figure 3**, the HG group exhibited a significantly higher proportion of late apoptotic cells compared with the NG group (p = 0.0266). Pre-treatment with either CCNPs or metformin significantly reduced the percentage of late apoptotic cells relative to the HG group. Notably, CCNPs exerted a dose-dependent protective effect, with CCNP3 producing the greatest reduction in apoptosis. In contrast, no significant difference in the proportion of early apoptotic cells was observed between the NG and HG groups (p = 0.1286).

The anti-apoptotic potential of CCNPs may be attributed to the strong antioxidant and anti-inflammatory properties of cinnamaldehyde (CA) [17]. CA has been shown to scavenge free radicals and upregulate endogenous antioxidant enzyme expression, thereby reducing oxidative stress [45]. Furthermore, CCNPs have been reported to enhance cellular glucose uptake and improve energy metabolism under hyperglycemic conditions, subsequently suppressing apoptotic signaling and favor cell survival [20,46].

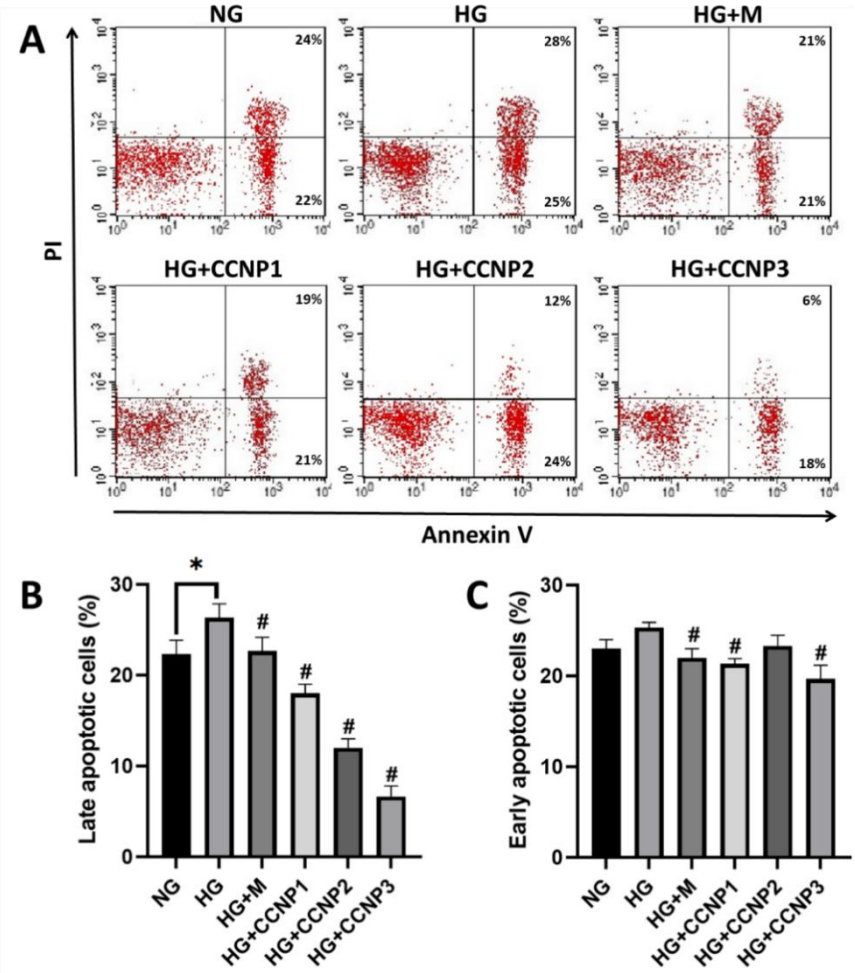

Figure 3 Effects of CCNPs on cellular apoptosis analyzed using Annexin V-PI flowcytometric assay, presented as (A) dot plots and (B,C) bar graphs representing mean±SD. NG: normal glucose/control; HG: high-glucose; M: metformin 50 μM; CCNP1-3: Cinnamaldehyde-chitosan nanoparticles at 12.5, 25, and 50 μM. *p < 0.05 vs. corresponding group; #p < 0.05 vs. HG group; n = 3.

To further elucidate the underlying mechanism, intracellular levels of PI3K and p-AKT were quantified by ELISA after 24 h of HG exposure (**Figures 4(A)** and **4(B)**). The HG group demonstrated decreased PI3K and p-AKT levels relative to NG group ($p < 0.05$), consistent with high-glucose induced impairment of the PI3K/AKT pathway. Pre-treatment with metformin or CCNPs counteracted these effects, showing elevated PI3K and p-AKT levels compared to the HG group. Notably, CCNP treatment at 50 μM (CCNP3) significantly increased both PI3K and p-AKT concentrations ($p < 0.05$). These findings indicate that CCNPs upregulate the PI3K/AKT signaling pathway in HG-treated fibroblasts.

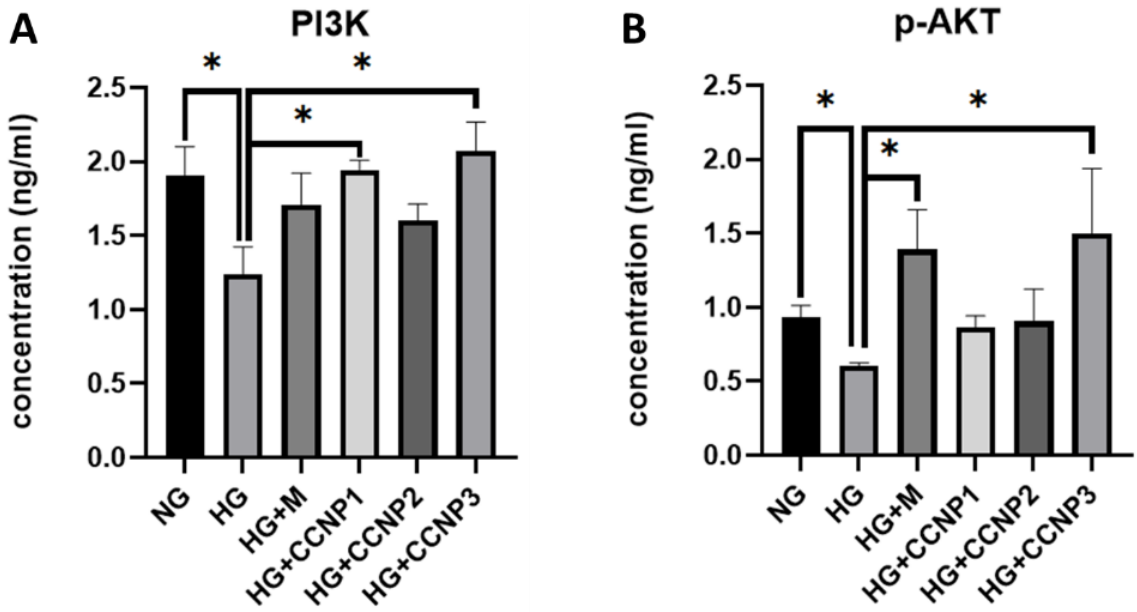

Figure 4 Effects of CCNPs on the concentration of PI3K (A) and p-AKT (B) protein in cell lysates. Bar graphs represent mean ± SD from 3 replicates. NG: normal glucose/control; HG: high-glucose; M: metformin 50 μM; CCNP1-3: Cinnamaldehyde-chitosan nanoparticles 12.5, 25, and 50 μM. *$p < 0.05$ as compared with the respective group; n = 3.

The PI3K/AKT pathway is a pivotal regulator of cell survival, metabolism, growth, and apoptosis [47]. Dysregulation of this pathway under hyperglycemic stress has been consistently linked to increased apoptotic activity in multiple cell types, including fibroblasts [48,49]. On the other hand, previous reports have demonstrated that the upregulation of the PI3K/AKT pathway can inhibit apoptosis caused by high-glucose environment in various cell types, supporting its role as a key cytoprotective axis [10,11,13]. In line with these reports, the present study demonstrates that CCNP treatment is associated with increased PI3K and phosphorylated AKT levels, concomitant with reduced apoptotic markers under hyperglycemic conditions.

Activation of PI3K and its downstream effector AKT promotes cell survival through phosphorylation-dependent mechanisms. AKT, a serine/threonine protein kinase, becomes fully active when phosphorylated at both Thr308 and Ser473 residues, although phosphorylation at either site alone can partially mediate downstream signaling [50]. Once activated, pAKT exerts anti-apoptotic effects by phosphorylating multiple target proteins, including BAD, FOXO, AMPK, and MDM2, which collectively inhibit pro-apoptotic signaling and promote metabolic adaptation under stress conditions [51]. The observed increase in p-AKT in CCNP-pre-treated fibroblasts is therefore consistent with a shift toward a pro-survival intracellular milieu.

Importantly, existing evidence indicates that cinnamaldehyde is the primary bioactive component responsible for PI3K/AKT modulation. Previous studies have demonstrated that CA exerts anti-

apoptotic effects in ischemia-reperfusion [17,18] and diabetic models through upregulation of phosphorylated PI3K and AKT, and that these effects are abolished by LY294002 (a selective PI3K inhibitor), confirming PI3K as a critical upstream mediator of CA anti-apoptosis effect [52]. These findings suggest that CA may either promote PI3K phosphorylation directly or modulate upstream signaling nodes that converge on PI3K activation. In addition, CA exhibits potent antioxidant activity, acting both as a direct radical scavenger and as an inducer of endogenous antioxidant defenses. CA directly scavenges radicals such as DPPH, superoxide, and nitric oxide, mainly by donating a hydrogen atom or an electron from its conjugated system to the radical, forming a more stable CA-derived radical and converting the aggressive radical into a non-radical species [53]. By reducing intracellular oxidative stress, CA may indirectly preserve PI3K/AKT signaling, as excessive ROS is known to impair kinase phosphorylation and promote apoptotic cascades. Additionally, CA has been shown to upregulate insulin receptor substrate-1 (IRS-1) in streptozotocin-induced diabetic rats, which facilitates PI3K recruitment and activation through canonical insulin-signaling mechanisms [20]. Complementing these biological data, our previous *in silico* analysis demonstrated that cinnamaldehyde can bind to predicted active or regulatory sites on PI3K catalytic subunits and AKT1/AKT2, raising the possibility of direct structural modulation of these proteins [22]. Nevertheless, these computational predictions have not yet been validated experimentally, and no biochemical evidence currently confirms direct phosphorylation of PI3K or AKT by CA.

Chitosan nanoencapsulation does not appear to directly activate PI3K/AKT signaling but instead confers pharmacokinetic and biophysical advantages that likely potentiate CA's intracellular actions. Encapsulation within chitosan nanoparticles protects CA from oxidative degradation and volatilization, enhances its aqueous stability, and enables sustained release, thereby prolonging cellular exposure [26]. Previous studies revealed that CCNPs generally show a biphasic release pattern, characterized by an initial burst release - typically accounting for approximately 25% - 60% of the encapsulated CA within the first 12 h - followed by a slower and more stable, diffusion-controlled release phase over the subsequent 12 - 36 h [27,36,54]. Importantly, the reported release kinetics of CA vary substantially across the literature and are highly dependent on nanoparticle formulation parameters, including chitosan molecular weight, crosslinking density, drug-loading efficiency, as well as the solvent system and experimental conditions used for *in vitro* release studies. This burst release might be attributed to the release of unencapsulated or poorly entrapped CA, as well as the diffusion of the encapsulated CA through the polymeric matrix. Although such burst release remains a formulation challenge, the subsequent controlled release phase may contribute to prolonged biological activity and sustained modulation of intracellular signaling pathways. Moreover, CA release from chitosan nanoparticles has been shown to be pH-dependent, with higher burst release observed under acidic conditions, reflecting accelerated diffusion and polymer relaxation in acidic environments [55].

Once released, the nanoscale size and positive surface charge of chitosan enhance the affinity of CCNP with negatively charged cell membranes and promote cellular uptake via adsorptive endocytosis [56]. Nonetheless, previous study have demonstrated that encapsulation with chitosan nanoparticles effectively enhances not only the bioavailability of the bioactive compound, but also its antioxidant capacity [57]. Therefore, eventhough a direct comparison with free cinnamaldehyde was not conducted in the present study, it is plausible that the observed cytoprotective effects of CCNPs are at least partially attributed to the improved intracellular delivery and sustained bioavailability of cinnamaldehyde conferred by the chitosan nanocarrier system.

Current standard therapies for diabetic wounds predominantly focus on correcting systemic and local factors, rather than directly addressing fibroblast perturbation which is essential in wound healing. In contrast, novel fibroblast-targeted strategies aim to restore impaired cellular survival and reparative capacity by correcting molecular and metabolic defects in diabetic fibroblasts [6,7]. In study, CCNPs integrate the intrinsic antioxidant and anti-apoptotic properties of CA with the enhanced cellular uptake, stability, and sustained bioavailability afforded by chitosan

nanoencapsulation. This combined pharmacological and delivery-based approach may offer a complementary strategy that directly supports fibroblast survival under hyperglycemic stress. Although direct comparisons with established clinical wound therapies were beyond the scope of this *in vitro* study, the observed attenuation of fibroblast apoptosis and partial restoration of PI3K/AKT signaling suggest CCNPs as a mechanistically distinct and potentially synergistic adjunct to standard diabetic wound treatment.

Nonetheless, several limitations of this study must be acknowledged. First, the experiments were conducted using a short-term *in vitro* hyperglycemia model which, while appropriate for investigating fibroblast responses to acute glucose stress, it does not fully capture the chronic and complex nature of diabetes *in vivo*. Second, although the cytoprotective effects of CCNPs were clearly demonstrated, a direct comparison with free cinnamaldehyde was not performed; therefore, the relative contribution of nanoencapsulation versus the intrinsic effects of CA cannot be quantitatively distinguished. Third, while increased PI3K and p-AKT levels support involvement of the PI3K/AKT pathway, the absence of pathway-specific inhibitors precludes definitive causal attribution. In addition, key formulation parameters such as encapsulation efficiency and release kinetics were not evaluated and warrant further optimization. Accordingly, future studies incorporating PI3K/AKT-specific inhibitors are required to confirm mechanistic involvement of this signaling axis. Moreover, comprehensive physicochemical characterization and in vivo investigations are needed to assess long-term efficacy, biodistribution, bioavailability, and potential toxicity of CCNPs within the complex diabetic wound model.

Conclusions

Cinnamaldehyde-chitosan nanoparticles (CCNPs) attenuated high-glucose-induced apoptosis in NIH-3T3 fibroblasts, an effect that appears to be associated with modulation of the PI3K/AKT signaling pathway. These findings provide preliminary in vitro evidence supporting CCNPs as a potential fibroblast-protective strategy under hyperglycemic conditions.

Acknowledgements

The authors would like to thank the Institute of Research and Community Services - Universitas Brawijaya, Indonesia for their financial support (1759.1.7/UN10.C20/2023).

CRediT author statement

Editya Fukata: Conceptualization, Methodology, Investigation, Data Curation, Formal analysis, Writing - Original Draft, Visualization; **Mohammad Saifur Rohman**: Methodology, Validation, Formal analysis, Writing - Review & Editing; **Aulanni'am**: Investigation, Data Curation, Visualization, Writing - Review & Editing; **Husnul Khotimah**: Investigation, Resources, Validation, Writing - Review & Editing; **Nik Ahmad Nizam Nik Malek**: Resources, Data Curation, Formal analysis, Writing - Review & Editing; **Agustina Tri Endharti**: Conceptualization, Supervision, Project Administration, Funding Acquisition, Writing - Review & Editing.

References

[1] International Diabetes Federation. IDF diabetes atlas, Available at: https://diabetesatlas.org/atlas/tenth-edition/, accessed October 2025.

[2] CMO Volpe, PH Villar-Delfino, PMF dos Anjos and JA Nogueira-Machado. Cellular death, reactive oxygen species (ROS) and diabetic complications. *Cell Death & Disease* 2018; **9(2)**, 119.

[3] SP Levick and A Widiapradja. The diabetic cardiac fibroblast: mechanisms underlying phenotype and function. *International Journal of Molecular Sciences* 2020; **21(3)**, 970.

[4] P Buranasin, K Mizutani, K Iwasaki, CPN Mahasarakham, D Kido, K Takeda and Y Izumi. High glucose-induced oxidative stress impairs proliferation and migration of human gingival fibroblasts. *PLoS One* 2018; **13(8)**, e0201855.

[5] A Perez-Favila, ML Martinez-Fierro, JG Rodriguez-Lazalde, MA Cid-Baez, M de J Zamudio-Osuna, Ma del R Martinez-Blanco, FE Mollinedo-Montaño, IP Rodriguez-Sanchez, R Castañeda-Miranda and I Garza-Veloz. Current

therapeutic strategies in diabetic foot ulcers. *Medicina* 2019; **55(11)**, 714.

[6] Y Liu, Y Liu, J Deng, W Li and X Nie. Fibroblast growth factor in diabetic foot ulcer: Progress and therapeutic prospects. *Frontiers in Endocrinology* 2021; **12**, 744868.

[7] Z Ma, Y Ding, X Ding, H Mou, R Mo and Q Tan. PDK4 rescues high-glucose-induced senescent fibroblasts and promotes diabetic wound healing through enhancing glycolysis and regulating YAP and JNK pathway. *Cell Death Discovery* 2023; **9(1)**, 424.

[8] X Chen, N Xie, L Feng, Y Huang, Y Wu, H Zhu, J Tang and Y Zhang. Oxidative stress in diabetes mellitus and its complications: From pathophysiology to therapeutic strategies. *Chinese Medical Journal* 2025; **138(1)**, 15.

[9] CY Huang, MY Ng, T Lin, YW Liao, WS Huang, CW Hsieh, CC Yu and CJ Chen. Quercetin ameliorates advanced glycation end product-induced wound healing impairment and inflammaging in human gingival fibroblasts. *Journal of Dental Sciences* 2024; **19(1)**, 268-275.

[10] S Bathina, NKV Gundala, P Rhenghachar, S Polavarapu, AD Hari, M Sadananda and UN Das. Resolvin D1 ameliorates nicotinamide-streptozotocin-induced type 2 diabetes mellitus by its anti-inflammatory action and modulating PI3K/Akt/mTOR pathway in the brain. *Archives of Medical Research* 2020; **51(6)**, 492-503.

[11] Y Dong, Y Xing, J Sun, W Sun, Y Xu and C Quan. Baicalein Alleviates Liver Oxidative Stress and Apoptosis Induced by High-Level Glucose through the Activation of the PERK/Nrf2 Signaling Pathway. *Molecules* 2020; **25(3)**, 599.

[12] T Soydaş, EY Saraç, S Çınar, G Yenmiş, S Doğan, S Solakoğlu, M Tunçdemir and GK Sultuybek. Effects of short-term high glucose on NIH/3T3 fibroblast proliferation, apoptosis, and collagen type I production. *Tıp Fakültesi Klinikleri Dergisi* 2019; **2(3)**, 91-95.

[13] W Xie, P Zhou, M Qu, Z Dai, X Zhang, C Zhang, X Dong, G Sun and X Sun. Ginsenoside re attenuates high glucose-induced RF/6A injury via regulating PI3K/AKT inhibited HIF-1α/VEGF signaling pathway. *Frontiers in Pharmacology* 2020; **11**, 695.

[14] AA Doyle and JC Stephens. A review of cinnamaldehyde and its derivatives as antibacterial agents. *Fitoterapia* 2019; **139**, 104405.

[15] K Yang, A Liu, A Hu, J Li, Z Zen, Y Liu, S Tang and C Li. Preparation and characterization of cinnamon essential oil nanocapsules and comparison of volatile components and antibacterial ability of cinnamon essential oil before and after encapsulation. *Food Control* 2021; **123**, 107783.

[16] R Karimirad, BS Inbaraj and BH Chen. Recent Advances on the analysis and biological functions of cinnamaldehyde and its derivatives. *Antioxidants* 2025; **14(7)**, 765.

[17] X Qi, R Zhou, Y Liu, J Wang, WN Zhang, HR Tan, Y Niu, T Sun, YX Li and JQ Yu. Trans-cinnamaldehyde protected PC12 cells against oxygen and glucose deprivation/reperfusion (OGD/R)-induced injury via anti-apoptosis and anti-oxidative stress. *Molecular and Cellular Biochemistry* 2016; **421(1)**, 67-74.

[18] B Zheng, J Qi, Y Yang, L Li, Y Liu, X Han, W Qu and L Chu. Mechanisms of cinnamic aldehyde against myocardial ischemia/hypoxia injury *in vivo* and *in vitro*: Involvement of regulating PI3K/AKT signaling pathway. *Biomedicine & Pharmacotherapy* 2022; **147**, 112674.

[19] CM Sena, A Pereira and RM Seiça. Cinnamaldehyde supplementation reverts endothelial dysfunction in rat models of diet-induced obesity: Role of NF-E2-related factor-2. *Antioxidants* 2023; **12(1)**, 82.

[20] ME Abdelmageed, GS Shehatou, RA Abdelsalam, GM Suddek and HA Salem. Cinnamaldehyde ameliorates STZ-induced rat diabetes through modulation of IRS1/PI3K/AKT2 pathway and AGEs/RAGE interaction. *Naunyn-Schmiedeberg's Arch Pharmacol* 2019; **392(2)**, 243-258.

[21] YF Chen, KJ Wu, CC Kuo and HY Tsai. Protection of Gueichih-Fuling-Wan on cerebral ischemia-induced brain injury in rodents is mediated by trans-cinnamaldehyde via inhibition of neuroinflammation and apoptosis. *Biomedicine* 2024; **14(2)**, 38-48.

[22] E Fukata, A Aulanni'am, MS Rohman, S Fakurazi, NANN Malek, Y Kawamoto and AT Endharti. *In silico* prediction of cinnamaldehyde on the PI3K/AKT pathway activator of anti-apoptotic potential. *Journal of Pharmacy & Pharmacognosy Research* 2025; **13(2)**, 565-577.

[23] DRA Muhammad, A Sedaghat Doost, V Gupta, MD bin Sintang, D Van de Walle, P Van der Meeren and K Dewettinck. Stability and functionality of xanthan gum-shellac nanoparticles for the encapsulation of cinnamon bark extract. *Food Hydrocolloids* 2020; **100**, 105377.

[24] L Wu, Y Meng, Y Xu and X Chu. Improved uptake and bioavailability of cinnamaldehyde via solid lipid nanoparticles for oral delivery. *Pharmaceutical Development and Technology* 2022; **27(10)**, 1038-1048.

[25] Q Liu, H Cui, B Muhoza, E Duhoranimana, S Xia, K Hayat, S Hussain, MU Tahir and X Zhang. Fabrication of low environment-sensitive nanoparticles for cinnamaldehyde encapsulation by heat-induced gelation method. *Food Hydrocolloids* 2020; **105**, 105789.

[26] B Muhoza, B Qi, JD Harindintwali, MYF Koko, S Zhang and Y Li. Encapsulation of cinnamaldehyde: an insight on delivery systems and food applications. *Critical Reviews in Food Science and Nutrition* 2023; **63(15)**, 2521-2543.

[27] SF Hosseini, J Ghaderi and MC Gómez-Guillén. Tailoring physico-mechanical and antimicrobial/antioxidant properties of biopolymeric films by cinnamaldehyde-loaded chitosan nanoparticles and their application in packaging of fresh rainbow trout fillets. *Food Hydrocolloids* 2022; **124**, 107249.

[28] P Subhaswaraj, S Barik, C Macha, PV Chiranjeevi and B Siddhardha. Anti quorum sensing and anti-biofilm efficacy of cinnamaldehyde encapsulated chitosan nanoparticles against Pseudomonas aeruginosa PAO1. *LWT* 2018; **97**, 752-759.

[29] J Xu, Q Lin, M Sheng, T Ding, B Li, Y Gao and Y Tan. Antibiofilm effect of cinnamaldehyde-chitosan nanoparticles against the biofilm of *Staphylococcus aureus*. *Antibiotics* 2022; **11(10)**, 1403.

[30] R Mu, H Zhang, Z Zhang, X Li, J Ji, X Wang, Y Gu and X Qin. Trans-cinnamaldehyde loaded chitosan based nanocapsules display antibacterial and antibiofilm effects against cavity-causing Streptococcus mutans. *Journal of Oral Microbiology* 2023; **15(1)**, 2243067.

[31] R Awaluddin, DA Nugrahaningsih and EN Solikhah. The concentration-dependent pro-fibrotic effect of metformin on LPS and high glucose induced fibroblast NIH 3T3 and macrophage RAW 264.7 cell co-culture. *The Medical Journal of Malaysia* 2020; **75(S1)**, 10-13.

[32] LK Chao, WT Chang, W Shih and JS Huang. Cinnamaldehyde impairs high glucose-induced hypertrophy in renal interstitial fibroblasts. *Toxicology and Applied Pharmacology* 2010; **244(2)**, 174-180.

[33] DV SepAlveda. Trichrome stain for diagnosis of amoebae in parasitology laboratory. *Global Journal of Medical Research* 2013; **13(K7)**, 7-12.

[34] V Sandhiya and U Ubaidulla. A review on herbal drug loaded into pharmaceutical carrier techniques and its evaluation process. *Future Journal of Pharmaceutical Sciences* 2020; **6(1)**, 51.

[35] J Hu, Y Zhang, Z Xiao and X Wang. Preparation and properties of cinnamon-thyme-ginger composite essential oil nanocapsules. *Industrial Crops and Products* 2018; **122**, 85-92.

[36] M Ji, X Sun, X Guo, W Zhu, J Wu, L Chen, J Wang, M Chen, C Cheng and Q Zhang. Green synthesis, characterization and *in vitro* release of cinnamaldehyde/sodium alginate/chitosan nanoparticles. *Food Hydrocolloids* 2019; **90**, 515-522.

[37] A Loquercio, E Castell-Perez, C Gomes and RG Moreira. Preparation of chitosan-alginate nanoparticles for trans-cinnamaldehyde entrapment. *Journal of Food Science* 2015; **80(10)**, N2305-N2315.

[38] LE Low, SP Siva, YK Ho, ES Chan and BT Tey. Recent advances of characterization techniques for the formation, physical properties and stability of Pickering emulsion. *Advances in Colloid and Interface Science* 2020; **277**, 102117.

[39] M Danaei, M Dehghankhold, S Ataei, F Hasanzadeh Davarani, R Javanmard, A Dokhani, S Khorasani and MR Mozafari. Impact of particle size and polydispersity index on the clinical applications of lipidic nanocarrier systems. *Pharmaceutics* 2018; **10(2)**, 57.

[40] Z Németh, I Csóka, R Semnani Jazani, B Sipos, H Haspel, G Kozma, Z Kónya and DG Dobó. Quality by design-driven zeta potential optimisation study of liposomes with charge imparting membrane additives. *Pharmaceutics* 2022; **14(9)**, 1798.

[41] NH Hoang, T Le Thanh, R Sangpueak, J Treekoon, C Saengchan, W Thepbandit, NK Papathoti, A Kamkaew and N Buensanteai. Chitosan nanoparticles-based ionic gelation method: A promising candidate for plant disease management. *Polymers* 2022; **14(4)**, 662.

[42] L Wu and R Derynck. Essential role of TGF-β signaling in glucose-induced cell hypertrophy. *Developmental Cell* 2009; **17(1)**, 35-48.

[43] FJ López-Hernández. Cell surface area to volume relationship during apoptosis and apoptotic body formation. *Cellular Physiology and Biochemistry* 2021; **55(S1)**, 161-170.

[44] ZE Sadeq, IJ Lafta and SA Lamburne. Interference with quorum sensing of *Klebsiella pneumoniae* by some plant extracts can affect the biofilm formation and antibiotic resistance. *Baghdad Science Journal* 2025; **22(4)**, 1234-1245.

[45] R Wang, S Li, H Jia, X Si, Y Lei, J Lyu, Z Dai and Z Wu. Protective effects of cinnamaldehyde on the inflammatory response, oxidative stress, and apoptosis in liver of *Salmonella typhimurium*-challenged mice. *Molecules* 2021; **26(8)**, 2309.

[46] R Zhu, H Liu, C Liu, L Wang, R Ma, B Chen, L Li, J Niu, M Fu, D Zhang and S Gao. Cinnamaldehyde in diabetes: A review of pharmacology, pharmacokinetics and safety. *Pharmacological Research* 2017; **122**, 78-89.

[47] HB Kumar, S Manandhar, E Rathi, SP Kabekkodu, CH Mehta, UY Nayak, SG Kini and KSR Pai. Identification of potential Akt activators: A ligand and structure-based computational approach. *Mol Divers* 2024; **28(3)**, 1485-1503.

[48] NF Sangweni, RA Mosa, PV Dludla, AP Kappo, AR Opoku, CJF Muller and R Johnson. The triterpene, methyl-3β-hydroxylanosta-9,24-dien-21-oate (RA3), attenuates high glucose-induced oxidative damage and apoptosis by improving energy metabolism. *Phytomedicine* 2021; **85**, 153546.

[49] J Wang, H Yang, C Wang and C Kan. Cyp2e1 knockdown attenuates high glucose-induced apoptosis and oxidative stress of cardiomyocytes by activating PI3K/Akt signaling. *Acta Diabetologica* 2023; **60(9)**, 1219-1229.

[50] T Pungsrinont, J Kallenbach and A Baniahmad. Role of PI3K-AKT-mTOR pathway as a pro-survival signaling and resistance-mediating mechanism to therapy of prostate cancer. *International Journal of Molecular Sciences*2021; **22(20)**, 11088.

[51] BD Manning and A Toker. AKT/PKB signaling: Navigating the network. *Cell* 2017; **169(3)**, 381-405.

[52] H Lan, Q Zheng, K Wang, C Li, T Xiong, J Shi and N Dong. Cinnamaldehyde protects donor heart from cold ischemia - reperfusion injury via the Pi3k/Akt/Mtor pathway. *Biomedicine & Pharmacotherapy* 2023; **165**, 114867.

[53] M Davaatseren, YJ Jo, GP Hong, HJ Hur, S Park and MJ Choi. Studies on the anti-oxidative function of trans-cinnamaldehyde-included β-cyclodextrin complex. *Molecules* 2017; **22(12)**, 1868.

[54] CL Barrera-Martínez, F Padilla-Vaca, I Liakos, HI Meléndez-Ortiz, GY Cortez-Mazatan and RD Peralta-Rodríguez. Chitosan microparticles as entrapment system for trans- cinnamaldehyde: Synthesis, drug loading, and in vitro cytotoxicity evaluation. *International Journal of Biological Macromolecules* 2021; **166**, 322-332.

[55] PR Sarjono, N Ngadiwiyana, E Fachriyah, I Ismiyarto, NBA Prasetya and K Khikmah. Encapsulation of cinnamaldehyde using chitosan: Stability, mucoadhesive and cinnamaldehyde release. *Jurnal Kimia Sains dan Aplikasi* 2018; **21(4)**, 175-181.

[56] N Aibani, R Rai, P Patel, G Cuddihy and EK Wasan. Chitosan nanoparticles at the biological interface: Implications for drug delivery. *Pharmaceutics* 2021; **13(10)**, 1686.

[57] ES Kim, Y Baek, HJ Yoo, JS Lee and HG Lee. Chitosan-tripolyphosphate nanoparticles prepared by ionic gelation improve the antioxidant activities of astaxanthin in the *in vitro* and *in vivo* model. *Antioxidants* 2022; **11(3)**, 479.